

FULL PAPER

Activation and diffusion of ammonia borane hydrogen on gold tetramers

Leopoldo Mejía¹ | Franklin Ferraro² | Edison Osorio² | Cacier Z. Hadad¹ 

¹Instituto de Química, Universidad de Antioquia, calle 67 No. 53-108, Medellín, Colombia

²Departamento de Ciencias Básicas, Universidad Católica Luis Amigó, Transversal 51A 67B 90, Medellín, Colombia

Correspondence

Cacier Z. Hadad, Instituto de Química, Universidad de Antioquia, Calle 70 No. 52-21, Medellín, Colombia.
Email: cacier.hadad@udea.edu.co

Funding information

Colciencias, via "El Patrimonio Autónomo Fondo Nacional de Financiamiento para la Ciencia, la Tecnología y la Innovación Francisco José de Caldas," Grant/Award Number: 111565842463; Conicyt, Chile, Grant/Award Number: REDES150042

Abstract

One of the most serious candidates for safe storage of high hydrogen densities is ammonia borane, AB. Likewise, one of the most versatile catalysts known is gold in the form of atomic clusters. Taking these elements into account, in this work a density functional theory -based study about initial activation, detachment, and diffusion of ammonia borane hydrogen on gold tetramer, as a catalyst model, is developed. It was found that the total process is exergonic and that the hydrogen diffusion occurs with very low energy barriers. The process has a hydrogen detachment energy barrier lower than the one of the uncatalyzed AB, and that is easily overcome by the energy expelled in the previous stage of formation of the initial activated species. Additionally, all the process is assisted by the fluxionality of the gold cluster, and occurs via a unique catalytically activated initial species, which contains a three-center simultaneous interaction at the catalytically activated zone.

KEYWORDS

ammonia borane, gold cluster catalyst, gold-fluxionality, theoretical study, three-center bonding

1 | INTRODUCTION

Research about new ways for practical, safe, and economically convenient storage and release of large quantities of hydrogen in small volumes is today a very important issue.^[1,2] Hydrogen has an energy content by mass almost three times superior to petroleum,^[3] is the most abundant substance in the universe, is source-independent, and its combustion product, water, is environmentally friendly. Additionally, the availability of activated hydrogen is highly relevant for a large number of reactions in the chemical industry, where reduction or hydrogenation are necessary steps.^[4,5] Among lightweight hydrogen storage materials, ammonia borane, AB (H_3BNH_3), is a substance that contains large amounts of hydrogen (a total of 19.6 wt.%),^[3] which is relatively easy to extract, either by direct or by assisted thermolysis,^[6,7] by catalyzed room temperature solvolysis,^[3,8-11] or by other methods.^[12-15] Additionally, AB can be easily and safely transported,^[16] because, on the one hand, is a relatively stable solid at room conditions,^[3,6,16] and is a substance soluble in many solvents, such as water, methanol, and tetraglyme.^[3,8-12]

It has been found that the use of transition metals as catalysts in the AB dehydrogenation has the advantage of avoiding the expenditure of large amounts of energy, necessary for the hydrogen release.^[7,16-18] Even, in some cases, the catalysis has emerged as a solution to diminish the unwanted by-products of hydrogen release.^[10,12,18] Transition metals of different nature, both noble and non-noble, as well as binary or tertiary combinations among them, have shown catalytic activity toward the extraction of hydrogen from AB.^[3,8-12,17,18] In the case of nanoparticles, the studies show that although some transition metals are better than others, the decrease in size (within certain limits and conditions^[19]) of the nanoparticles of the used metal and the increase in their structural disorder, are factors that greatly enhance their catalytic capabilities, regardless of the metal nature.^[3,10] Even the modulation of these factors has allowed the transformation of catalytically inactive metals into active ones.^[3,10] This is an indication of compliance, in this case, of a known usual fact in the field of catalysis: the catalytic activity increases with the number of structural corners and edges on the catalyst surface, where the active sites consist in low coordinated atoms, or subjected to interaction with its neighbors resulting in less energy-favored geometries.^[4,20]

The initial step in metal-catalyzed dehydrogenation of AB, is the weakening of the boron-hydrogen bond, through the formation of a metal-hydrogen and metal-boron binding interactions,^[12,21,22] which has been also described as an agnostic interaction.^[23] After that, according to the conditions and the dehydrogenation method used, the mechanisms can vary. This not only applies to the dehydrogenation assisted

by metal complexes in organic solvents,^[12,22,23] but also to metal-catalyzed hydrolysis,^[21] where it was traditionally believed in another initial mechanism.^[3,8,20]

On the other hand, in the field of catalytic hydrogenation reactions, one important step is the generation of activated hydrogen. This is traditionally achieved through the catalytic dissociation of molecular hydrogen using different type of catalysts.^[4,24,25] It has been found that especially efficient has been the use of small catalytic particles, such as nanoparticles, small metallic clusters, and even individual atoms, supported on different type of surfaces.^[4,25-28] In the case of metallic clusters supported on surfaces, one relevant sequence of catalytic processes starts with the hydrogen dissociation, followed by the diffusion of hydrogen atoms through the metallic clusters, and finally, the induced spillover of the hydrogen atom over the surface, wherein the hydrogen-surface interaction is weak enough to allow easy access of reactive hydrogen.^[24,25,28,29] In this regard, gold has been used both, as noble metal cluster catalyst,^[25,29] or as support surface.^[28] In fact, since the discovery of catalytic properties of gold in the form of nanoparticles and small clusters,^[30] this noble metal has been one of the most studied as a catalyst. One very interesting property of gold clusters is the structural fluxionality, namely, the interconversion among cluster structures, which, remarkably, can also influence catalytic processes.^[31-34] Gold fluxionality is due to the habitual existence of large amount of structures very close in energy to the global minimum. This process occurs so easily that has been possible to observe it directly and in real time over surfaces.^[28]

In view of all the elements exposed above it could be interesting to work out the following questions: How feasible is the removal of a hydrogen atom from AB by using a gold cluster, and how easy is the further diffusion of this atom on the cluster? What is the nature of the bonding during the initial AB catalytic activation (the formation of “adsorption” complexes)? Is the catalytic process assisted by the fluxionality of the catalyst? In this work, we offer a computational study to contribute in the answer of these questions by using neutral gold tetramer as a representative cluster. Au₄ has the advantage of being a much-studied system from theoretical and experimental point of views.^[35-38] For example, it has been used as a viable and representative model of supported small clusters for dehydrogenation reactions.^[25,29] Additionally, Au₄ is small enough to be studied at high theory levels, but is of sufficient size to present the fluxionality phenomenon.

2 | COMPUTATIONAL METHODS

A crucial first stage is to find the most energetically favorable initial adduct resultant of the interaction between ammonia borane and the catalyst, that is, finding the initial activated species. The subsequent catalytic transformations would start from this species. To achieve this, it is convenient to have a methodology for a sufficiently exhaustive scan of the configurations space for the possible interactions between AB and Au₄, especially in low-energy areas. We have found that stochastic-based search of suitable candidate structures for the mutual AB and Au₄ spatial disposition, and their subsequent gradient-based optimizations, has proven to be a very successful combination of methodologies. Among stochastic-based methods, ASCEC^[39,40] has demonstrated to be very effective, both for atomic and molecular clusters of diverse nature.^[33,39-44] ASCEC is a simulated annealing algorithm in which the Metropolis criterion has been modified in such a way that it is possible to ensure exhaustive scans, moving down from high energy areas to areas of the lowest possible energies for the studied adducts. In the present work, for the ASCEC calculations, the AB and Au₄ respective centers of mass were located at the center of cubic cages of 4 to 6 Å of edge, from which the respective random walks started. For the evaluation of the singlet-point energies for each AB and Au₄ stochastic geometrical disposition, we used the HF/LANL2DZ model chemistry by means of GAUSSIAN 09,^[45] which is called during ASCEC routines. For the subsequent gradient-based geometry optimizations of the candidate structures (produced by ASCEC), the ZORA (Zeroth-Order Regular Approximation) scalar relativistic PW91/TZ2P level of theory was employed, using the ADF2013.02 program.^[46] The ZORA scalar relativistic methodology incorporates relativistic effects in the Hamiltonian and is practically gauge invariant and especially suitable for valence orbitals.^[47] The PW91 functional is a generalized gradient approximation (GGA), in which the functional depends on local density and its gradient. This combines exchange and correlation functionals, developed by Perdew and Wang.^[48,49] The TZ2P basis set are, as all the basis used in ADF, Slater-type orbitals (STOs). They include Triple-zeta with two polarization functions as implemented in ZORA/TZ2P basis set files of ADF program.^[46] For our systems, we use the all electrons basis set. The stochastic-based search of candidate initial configurations (ASCEC) is only a first selection filter and, therefore, it is not necessary nor efficient to use a more sophisticated level of theory for singlet-point energy evaluations. The LANL2DZ basis set employed in ASCEC includes pseudopotentials to take into account the relativistic effects in gold atoms. These effects are much better considered by the ZORA scalar relativistic method, used in the gradient-based optimization stage. Our previous studies about the C₂H₂-Au₇ system^[33] yielded excellent results with this combination of computational levels of theory, which were in agreement with several experimental evidences about the systems Au₇ and C₂H₂.^[33]

The respective isolated AB and Au₄ lowest energy structures at PW91/TZ2P level of theory were used as initial geometries in our calculations. For the AB molecule, the staggered conformation is the lowest energy isomer. The ZORA-PW91/TZ2P BH, BN, and NH bond lengths are 1.214, 1.651, and 1.021 Å, respectively, which agrees very well with the experimental ones for the AB in the gas phase: 1.216, 1.646, and 1.024 Å, respectively.^[6]

Contrary to the case of the isolated AB molecule, in which only one geometrical shape is possible, and in which the conformational isomerism does not introduce differences for the interaction with the catalyst, in the case of Au₄ it is necessary to pay special attention to properly locate its lowest energy configurations. In fact, for Au₄ there are two different geometrical motifs, very close in energy to each other (see Figure 1A).^[35] The

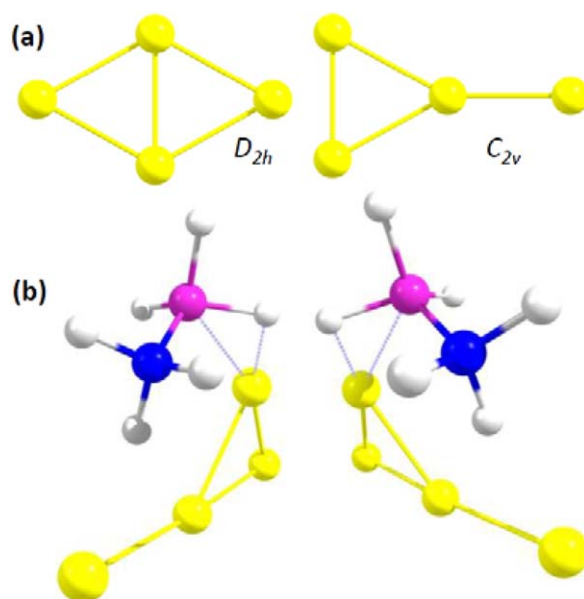


FIGURE 1 A, The two lowest energy structures of Au₄: the D_{2h} rhomboid-like geometry (left) is the global minimum, which is at 0.041 eV below the C_{2v} Y-like geometry (right). B, The lowest energy structures for the initial interaction of AB and Au₄. They correspond to optical isomers having, obviously, the same energy. The four structures of this figure correspond to singlet spin states at ZORA scalar relativistic PW91/TZ2P level of theory (For details see Computational methods)

global minimum corresponds to a D_{2h} rhomboid-like geometry, and the second most stable geometry to a C_{2v} Y-like geometry, at only 0.041 eV above; both structures at singlet spin state. The theoretical description that the lowest energy isomer is the D_{2h} rhomboid one (Figure 1A) coincides with experimental and theoretical findings for neutral gold tetramer.^[37,38] Likewise, the theoretical descriptions also found that this structure is followed by some hundredths of eV by the C_{2v} Y-like structure (see e.g., Ref. 37). Additionally, multiconfiguration self-consistent-field (MCSCF), followed by multireference configuration interaction (CI) calculations predict that the peripheral Au–Au bond lengths for the rhomboidal geometry is of 2.69 Å,^[36] which is the same value found by us at ZORA scalar relativistic PW91/TZ2P level of theory (2.688 Å).

The final structures, resulting from the combination ASCEC/optimizations, were reoptimized at PW91/Def2TZVP level of theory, which was also used to obtain the energy profiles for hydrogen release and diffusion on Au₄, and studies about the nature of the initial AB–Au₄ equilibrium species (all of them using GAUSSIAN 09 suit of programs^[45]).

Def2TZVP is a basis set which incorporates scalar relativistic effects through effective core potentials (60 inner electrons for the Au case). For the remaining electrons it uses valence triple-zeta polarization gaussian functions.^[50,51]

For the systems of our interest, the PW91/Def2TZVP model chemistry turns out to be pretty much equivalent to the PW91/TZ2P one. For example, the changes in the AB–Au₄ bond lengths in going from the structure optimized with PW91/TZ2P to the one optimized with PW91/Def2TZVP, were, in average, of only 0.14% (see Appendix 1 in the Supporting Information). Conversely, for the AB isolated structure the geometrical parameters using the PW91/Def2TZVP model chemistry are very close to the experimental ones (named above; 1.216, 1.646, and 1.024 Å for BH, BN, and NH bond lengths, respectively^[6]). They are 1.215, 1.648, and 1.023 Å, for BH, BN, and NH bond lengths, respectively. Again, those values are so close to the ZORA-PW91/TZ2P ones, listed above.

All the above facts give us confidence in the correctness of the sequence of methodological approaches used in our systems.

Appendix 2 summarizes the comparison of our calculations for the species, AB, Au₄, and AB–Au₄ with the data of the literature, when it is possible.

The construction of the energy profile for the hydrogen release and diffusion on Au₄ were carried out by means of one of the following strategies for each of its elementary steps: (a) Searches for the possible transition state, TS, followed by calculations of intrinsic reaction coordinate, IRC. The TSs were found by relaxed scan tests (geometric optimizations at PW91/Def2TZVP level, after the sequential variation of some coordinate of the system), and posterior optimizations of the candidates structures at PW91/Def2TZVP level using Broyden algorithm.^[52] Calculations of IRCs were carrying out by the Hessian based predictor-corrector integrator algorithm,^[53] starting from the found TS. (b) Providing the reactant and a possible product (taking from optimization of some candidate structure), search for the TS using the Synchronous Transit-Guided Quasi-Newton Method.^[54] and then reoptimization of the TS structure at PW91/Def2TZVP level using Broyden algorithm.^[52]

Calculations were done at singlet spin states; we compared the relative energies of the resultant structures with respect to similar or different structures at higher spin multiplicities, finding that the singlet structures are always those with the lowest energies. Conversely, the characterization of all the structures as local or global minima (no negative eigenvalues of the Hessian matrix) or as transition states (one negative eigenvalues of the

Hessian matrix), were done with frequency calculations at the same level of theory of optimizations at each stage of calculations. Gibbs free energies at 298.15 K were estimated by standard statistical thermodynamics for ideal gases as is implemented in frequency calculations routines of GAUSSIAN 09.^[45] Cartesian coordinates for all resultant structures are set forth in the Appendix 3 of the Supporting Information.

The nature of bonding for the initial activated species was examined by a combination of Natural Bond Orbital, NBO,^[55,56] Quantum Theory of Atoms in Molecules, QTAIM,^[57] and Adaptive Natural Density Partitioning, AdNDP,^[58] methodologies. Wiberg bond indices, natural charges and second-order perturbation theory analysis of Fock matrix were calculated along the lines of the NBO 6.0 program.^[56] Wiberg bond indices^[59] correspond to the off-diagonal density matrix elements squares sum between the atom pairs of the system, being, in this case, the requested orthonormal basis the natural atomic orbitals.^[56] They are used as approximations to share-like or covalent bond orders. In rough terms, Wiberg bond indices close to 1, 2, etc., indicate single, double, etc., pure covalent bonds, respectively. Second-order perturbation theory analysis of Fock matrix quantitatively estimates donor (bond)-acceptor (anti-bond) interactions in the NBO basis.^[55] Molecular graphs for the activated AB—Au₄ species, within the QTAIM, framework,^[57] were obtained by means of AIMALL code.^[60] In very rough terms, molecular graphs consist in molecular structures showing “bond paths,” that is, the lines of highest electron density joining the atomic centers. The presence of “bond paths” indicates some degree of interaction. Less known to the above is the Adaptive Natural Density Partitioning, AdNDP, method,^[58] which consists in the partitioning of the electronic density into elements of *n* center-two electrons, including core electrons and lone pairs. In this method, calculations are carrying out taking into account the lowest possible number of atomic centers per electron pair. AdNDP calculations were carrying out using the Multiwfn program.^[61]

3 | RESULTS AND DISCUSSIONS

3.1 | AB activation, hydrogen release and diffusion, and gold cluster-fluxionality

Taking into account the two lowest energy structural isomers for the Au₄ cluster (Figure 1A) and the AB molecule in its lowest energy conformation (staggered), the ASCEC stochastic-based search process for the mutual most favorable geometric dispositions of Au₄ and AB, gave 240 candidate structures. The subsequent ZORA scalar relativistic PW91/TZ2P gradient-based geometrical optimizations gave only two structures with positive lowest vibrational frequencies, that is, only two minima in the singlet AB—Au₄ ZORA-PW91/TZ2P potential energy surface. These structures turned out to be optical isomers to each other (Figure 1B). The fact of having found optical isomers is a sign that our process of PES scanning was very exhaustive. The result that only one type of activated complex (any of the two isomers) is obtained for the interaction between AB and Au₄, was corroborated with some independent scan tests for the mutual approach between Au₄, and AB, at the same and at other different level of theory (See Appendix 4 in the Supporting Information). In these tests, it is observed that the same equilibrium geometry, with respect to the ZORA-PW91/TZ2P one, are always reached for the interaction between AB and Au₄. Additionally, these tests allowed verifying that the AB and Au₄ mutual approach occurs without the existence of any energy barrier. This lack of energy barrier has been described before for the energy profiles of other AB/(metal catalyst) systems.^[17,23] Probably it is because the first contact between AB and Au₄ occurs between a hydridic-like H atom (connected to boron) and a very reactive electrophilic gold atom at a gold cluster vertex (e.g., the Au atoms of the above and below of the rhomboid D_{2h} cluster in Figure 1A, in which the LUMO orbitals are predominantly located^[35]).

In summary, the initial adducts of Figure 1B are the most likely structures for the interaction of Au₄ and AB, and are the suitable starting points for the subsequent dehydrogenation transformations.

What immediately can be observed in Figure 1B is that the initial interaction occurs by the side of the AB boron atom, and that the gold cluster geometry changed with respect to the initial one due to the activation process. With respect to the first observation, it is relevant to say that our calculations showed that the molecule of AB flips over when it is initially oriented with the nitrogen atom directed toward the gold cluster. About the second observation (by comparing the structures of Figure 1A,B), it can be appreciated that in the catalytically activated complex, the Au₄ isomer adopts a deformed geometrical configuration, whose shape is close to that of the C_{2v}, Y-like Au₄ isolated structure, regardless of whether the optimization starts from the C_{2v} or from the D_{2h} structure for the isolated Au₄ species. This is the first sign of the effects of the fluxionality of gold clusters referred to in the introduction of this article.

The results of the kinetic feasibility evaluation for the detachment and diffusion of hydrogen on gold tetramer are expressed in Figure 2. The showed energy profile contains the most probable path for AB initial activation, one hydrogen detach, and hydrogen diffusion on the catalysts. The indicated quantities correspond to the absolute value of the difference between the energy of two successive species in the profile. That the energy is released or absorbed in each elementary step can be deduced by going from left to right in the profile. The values without parentheses correspond to the ZPE-corrected electronic energy gaps, and the values in parentheses to Gibbs free energy gaps at 298.15 K, in the framework of Boltzmann statistics. The ZPE-corrected electronic energy values refer to a molecular system that does not rotate, that does not translate, that is only in its ground vibrational state, and that is not subject to collective entropic effects. This situation can be a first approximation to a cluster supported on (fixed to) some solid surface, which is the case of heterogeneous catalysis, but would not be good model for a homogeneous catalysis, either in a solvent or in the gaseous state. On the contrary, when calculating changes of Gibbs free energies, we account for the omitted degrees of freedom and

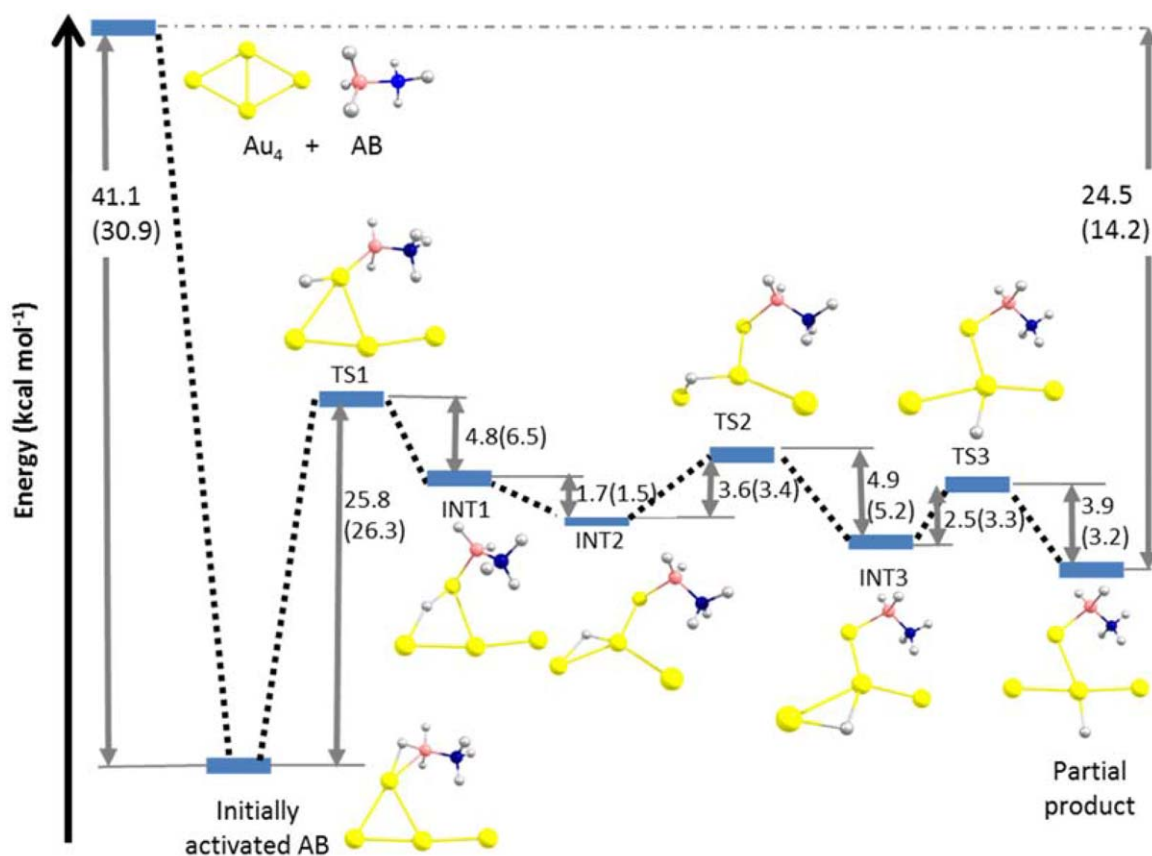


FIGURE 2 Energy profile for the AB initial activation, detachment and diffusion of hydrogen on gold tetramer. The indicated gaps correspond to ZPE-corrected electronic energies and, in parenthesis, to Gibbs free energies (298.15 K), all in kcal mol⁻¹. Calculations at singlet spin state and at PW91/Def2TZVP level of theory (For details see Computational methods)

we could consider the results as a first approximation to homogeneous catalysis. Of course, this has the limitations of omitting solvent effects and of being framed in Boltzmann statistic for the ideal system.

Inspecting Figure 2, first, it is observed that the process of AB initial activation, or “adsorption” stage, releases a ZPE-corrected electronic energy, E_{ZPE} , of 41.1 kcal mol⁻¹, and a Gibbs free energy, ΔG_{298} , of 30.9 kcal mol⁻¹, which implies electronic and geometric changes, and great influence of entropic changes (in going from two species, AB and Au₄ to one species, AB–Au₄). As can be seen in the figure, these quantities would be sufficient to drive the subsequent processes of detachment and diffusion of hydrogen. Starting from the AB–Au₄ initial adduct, the AB hydrogen detach has energy barriers of $E_{\text{ZPE}} = 25.8$ kcal mol⁻¹, and $\Delta G_{298} = 26.3$ kcal mol⁻¹, and leads to the transition state TS1. These energy barriers implicate a considerable reduction with respect to the ones for the ammonia borane isolated molecule. For example, for the ZPE-corrected electronic energy it means a reduction of 68.6% for B–H cleavage and of 19.7% for N–H cleavage (See Appendix 5 in Supporting Information). The N–H cleavage is the main one related to the thermal release of hydrogen,^[17] and the B–H cleavage to the catalytic process analyzed here. The transition state TS1 is characterized by the tendency of the hydrogen atom to move toward the interaction with a second gold atom, leading, in two steps, to a species where the hydrogen acts as a bridge between two gold atoms and in which the boron atom is directly bonded to a gold atom (intermediate state structure INT2, through INT1). The structure INT2 easily transforms into its structural isomer INT3, through the transition state TS2, for which it must traverse a small energy barrier of $E_{\text{ZPE}} = 3.6$ kcal mol⁻¹ (and of $\Delta G_{298} = 3.4$ kcal mol⁻¹). Finally, to reach the last species, in which the hydrogen atom is stabilized, and is far from the boron atom, INT3 must pass through the transition state TS3, which is only $E_{\text{ZPE}} = 2.5$ kcal mol⁻¹ ($\Delta G_{298} = 3.3$ kcal mol⁻¹) more energetic than INT3.

Clearly, the “rate-determining step” corresponds to the initial break of the BH bond, leading to the transition state TS1. This process has a non-negligible energy barrier, but which is lesser than the one released in the initial AB activation process (AB “absorption”). Therefore, no extra thermal energy would be required for the hydrogen detachment and migration. In other words, the net barrier of hydrogen detachment is negative, both in terms of ZPE-corrected electronic energy and in terms Gibbs free energy.

Finally, and in general terms, Figure 2 indicates that the diffusion of a hydrogen atom on gold tetramer occurs with very low energy barriers, that is, quite easily. Also indicates that, again, the process occurs with a great geometric flexibility of the gold cluster, due to the Au₄ fluxionality, which would facilitate the hydrogen diffusion.

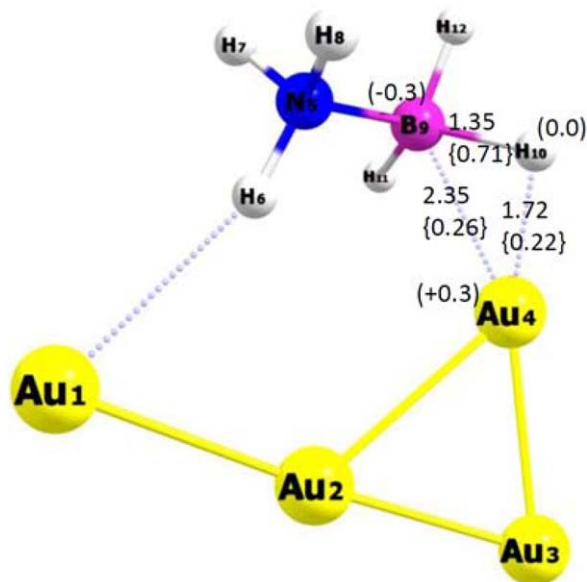


FIGURE 3 Distances in Å and Wiberg bond indexes (in brackets, below each distance) between interacting atoms in the initial activated species. In parenthesis, next to each interacting atom, are the natural atomic charges. Calculations at singlet spin state and at PW91/Def2TZVP level of theory

3.2 | Nature of bonding during the catalytic activation

Figure 3 shows natural atomic charges, distances and Wiberg bond indexes for interacting atoms in the initial AB—Au₄ adduct. At the main area of our interest, we can appreciate some degree of simultaneous interaction among the three involved atoms, B9, H10, and Au4. First, there are some weak shared-like character in the interactions between the atoms of the Au4—H10 and Au4—B9 pairs, expressed by the small values of the Wiberg bond indexes, 0.22 and 0.26, respectively. The Au4—B9 interaction could be reinforced at some extent by ionic-like attraction due to the charge separation between the opposed natural charges of boron (−0.3) and gold (+0.3). The presence of small bonding indexes between the Au4—H10 and Au4—B9 pairs is in line with their internuclear distances. In effect, Hydrogen, Boron, and Gold have atomic radii of about 0.53, 0.87, and 1.74 Å,^[62] and single bond covalent radii of about 0.32, 0.85, and 1.24 Å,^[63] respectively. These values give 2.27 (1.74 + 0.53) and 2.61 (1.74 + 0.87) Å for the Au—H and Au—B interatomic distances, respectively; and 1.56 (1.24 + 0.32) and 2.09 (1.24 + 0.85) Å for the Au—H and Au—B covalent bond lengths, respectively. The Au4—H10 and Au4—B9 distances in Figure 3 are 1.72 and 2.35 Å, respectively, which are within the reported interatomic and covalent values. Therefore, the Au—H and Au—B contacts in the activated AB—Au₄ species effectively are bonding interactions.

This degree of intermolecular bonding is accompanied by a weakening of the B9—H10 original bond. The B9—H10 bond length and Wiberg bond index of the isolated AB molecule are 1.22 Å and 0.98, respectively. By contrast, these values for the activated AB—Au₄ species are 1.35 Å and 0.71, respectively, showing the tendency toward the catalytic dehydrogenation.

It is interesting to examine these interactions from other theoretical point of views. The molecular graph for the initial activated AB—Au₄ species (see Appendix 6 in the Supporting Information), within the QTAIM framework, shows the presence of a bond path for the Au4—H10 interaction, but not for the Au4—B9 interaction. However, as we have reported in another case,^[64] there is a pronounced curvature of the bond paths toward the Au4—B9 internuclear region, which denote certain degree of Au—B interaction via other atoms (multicenter interactions). In fact, second-order perturbation theory analysis of Fock matrix within the NBO scheme^[65] predicts an interaction between the B9—H10 bonding localized orbital (donor) and the Au4—Au3 antibonding localized orbital (acceptor). This interaction is accompanied by a retro-donation from a lone electron pair (located in a d orbital) of the Au4 atom toward the B9—H10 antibonding orbital. Even though the NBO Lewis-based pair wise scheme seems not so suitable for this type of problem where we have the presence of a heavy transition metal and a catalytically activated species, we see that reaches to disclose the catalytic activation itself and the simultaneous interaction among several centers. A more suitable scheme, which allows the possibility of the simultaneous interaction among several atoms, is the AdNDP procedure (see Computational Methods).^[58] Figure 4 shows the relevant bonding in a sequence consisting of three stages for the activation reaction. Vertically, in the sequence of central images B, E, and H, it is depicted the changes in bonding that involve the three atoms of interest. In the image B there is still no significant interaction between AB and Au₄. In that picture it is depicted a relevant 2 center-2 electrons bond between H and B. Parallel, in images A and C, the intramolecular bonding in the gold tetramer is shown and consists in two bonds, each of 3 center-2 electrons.

In the image E, in where AB and Au₄ are closer to each other, it has already formed a 3 center-2 electrons bond among atoms H, B, and Au. The gold tetramer and its three center bonds have begun to deform (images D and F). Once the activated AB—Au₄ species is formed, the three center Au, H, B bond is in its final form (image H) and the bonds in the catalyst have changed into two combinations, one consisting in a 3 center-2 electron bond (image I) and the other in a 2 center-2 electron bond (image G).

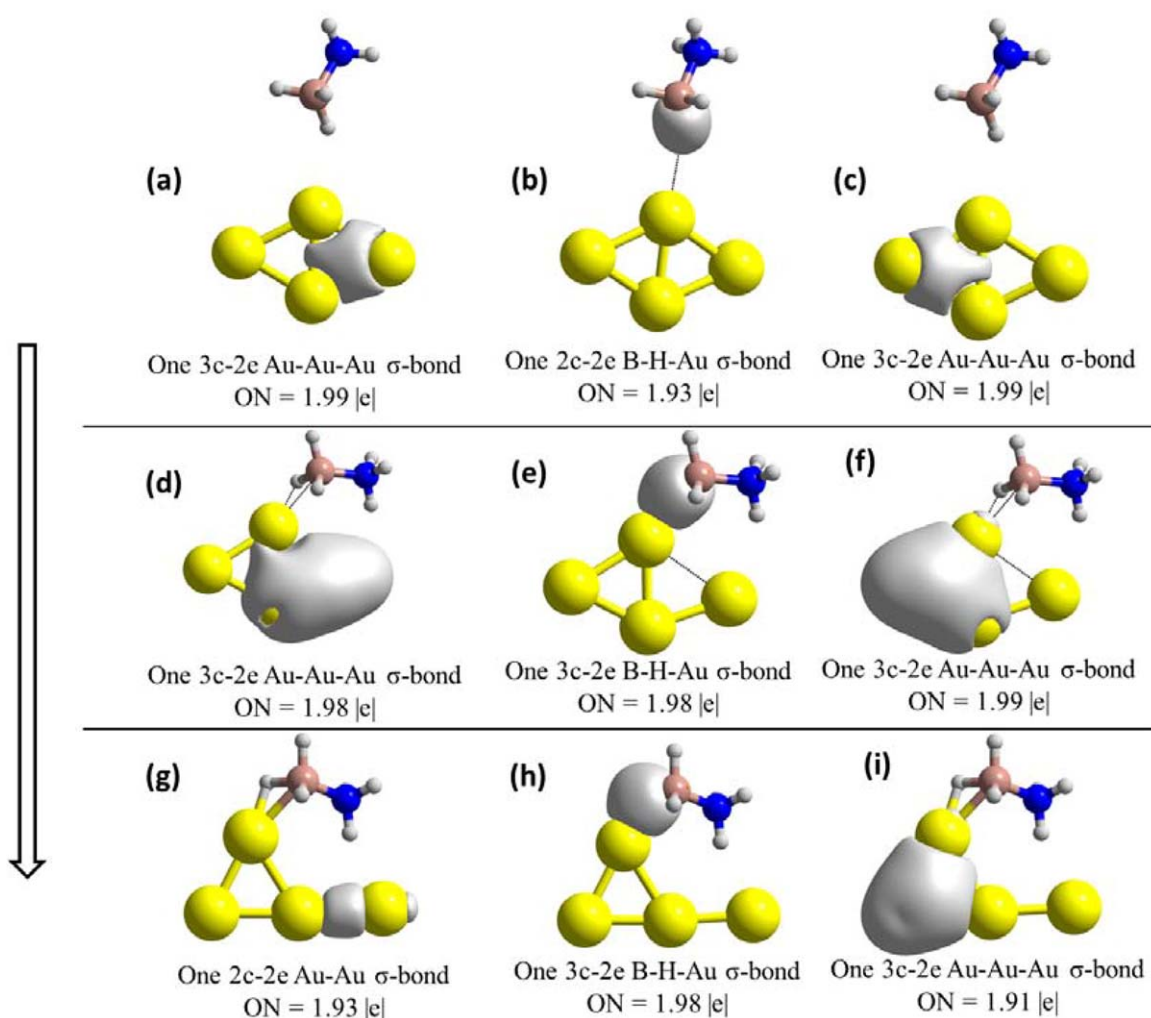


FIGURE 4 Multiple bonding in a sequence consisting of three stages for the AB activation by gold tetramer. A-C, images show the bonding scheme among relevant atoms in each noninteracting species, Au₄ and AB. D-F, images show a snapshot when AB is very close to Au₄. D-F, images correspond to the relevant multicenter-bonding when the activated species has already formed. nc: *n*-center (*n* = 2, 3), 2e: two electrons. ON: electronic occupation number

4 | CONCLUSIONS

The initial activation of ammonia borane by gold tetramers occurs by the side of boron through a hydridic-like hydrogen atom. This results in an initial AB–Au₄ adduct which contains a simultaneous hydrogen–boron–gold three-center interaction at the catalytically activated zone. This initial process occurs with change of catalyst geometry due to the Au₄ fluxionality. The initial activated species consists of two structures, which are mutual optical isomers. They are the unique, the most likely structures for the interaction between Au₄ and AB. They are the suitable starting points for the subsequent dehydrogenation transformations.

Both the electronic energy profile and the Gibbs free energy profile indicate that the labile hydrogen of the AB–Au₄ initial adduct is prone to being detached and would diffuse on the cluster with ease. The energy needed for this process would be completely taken from the energy released in the initial AB activation by Au₄. In fact, the whole process is spontaneous and has no effective or net energy barriers, but only internal energy barriers. The hydrogen diffusion occurs with a considerable change of catalyst geometry, due to the Au₄ fluxionality, which clearly assist the process.

ACKNOWLEDGMENTS

C.Z.H. is grateful to Colciencias, via “El Patrimonio Autónomo Fondo Nacional de Financiamiento para la Ciencia, la Tecnología y la Innovación Francisco José de Caldas” (111565842463), and to Conicyt, Chile, through REDES150042.

CONFLICT OF INTEREST

The authors declare that they have no conflict of interest.

ORCID

Cacier Z. Hadad  <http://orcid.org/0000-0002-2799-301X>

REFERENCES

- [1] L. Klebanoff, *Hydrogen Storage Technology: Materials and Applications*, CRC Press Taylor & Francis group, Boca Raton, Florida **2016**.
- [2] G. W. Crabtree, M. S. Dresselhaus, M. V. Buchanan, *Phys. Today* **2004**, *57*, 39.
- [3] H-L. Jiang, Q. Xu, *Catal. Today* **2011**, *170*, 56.
- [4] J. Hagen, *Industrial Catalysis*, 2nd ed., Wiley-VCH Verlag GmbH & Co, Weinheim, Germany **2006**.
- [5] J. A. Ritter, A. D. Ebner, *Sep. Sci. Technol.* **2007**, *42*, 1123.
- [6] C. R. Miranda, G. Ceder, *J. Chem. Phys.* **2007**, *126*, 184703.
- [7] A. Al-Kukhun, H. T. Hwang, A. Varma, *Ind. Eng. Chem. Res.* **2011**, *50*, 8824.
- [8] M. Chandra, Q. Xu, *J. Power Sources* **2006**, *156*, 190.
- [9] D. Sun, V. Mazumder, O. Metin, S. Sun, *ACS Catal.* **2012**, *2*, 1290.
- [10] H. Lu, Q. Yao, Z. Zhang, Y. Yang, X. Chen, *J. Nanomater.* **2014**, **2014**, ID 729029.
- [11] W. Chen, J. Ji, X. Feng, X. Duan, G. Qian, P. Li, X. Zhou, D. Chen, W. Yuan, *J. Am. Chem. Soc.* **2014**, *136*, 16736.
- [12] A. Rossin, M. Peruzzini, *Chem. Rev.* **2016**, *116*, 8848.
- [13] A. Gutowska, L. Li, Y. Shin, C. M. Wang, X. S. Li, J. C. Linehan, R. S. Smith, B. D. Kay, B. Schmid, W. Shaw, M. Gutowski, T. Autrey, *Angew. Chem. Int. Ed. Engl.* **2005**, *44*, 3578.
- [14] M. E. Bluhm, M. G. Bradley, R. Butterick, III, U. Kusari, L. G. Sneddon, *J. Am. Chem. Soc.* **2006**, *128*, 7748.
- [15] Z. Li, G. Zhu, G. Lu, S. Qiu, X. Yao, *J. Am. Chem. Soc.* **2010**, *132*, 1490.
- [16] T. B. Marder, *Angew. Chem. Int. Ed. Engl.* **2007**, *46*, 8116.
- [17] T. He, J. Wang, G. Wu, H. Kim, T. Proffen, A. Wu, W. Li, T. Liu, Z. Xiong, C. Wu, H. Chu, J. Guo, T. Autrey, T. Zhang, P. Chen, *Chemistry* **2010**, *16*, 12814.
- [18] T. He, Z. Xiong, G. Wu, H. Chu, C. Wu, T. Zhang, P. Chen, *Chem Mater.* **2009**, *21*, 2315.
- [19] H. Ma, Ch. Na, *ACS Catal.* **2015**, *5*, 1726.
- [20] Q. Xu, M. Chandra, *J. Power Sources* **2006**, *163*, 364.
- [21] W. Chen, D. Li, Z. Wang, G. Qian, Z. Sui, X. Duan, X. Zhou, I. Yeboah, D. Chen, *AIChE J.* **2017**, *63*, 60.
- [22] R. J. Keaton, J. M. Blacquiere, R. T. Baker, *J. Am. Chem. Soc.* **2007**, *129*, 1844.
- [23] S-K. Kim, W-S. Han, T-J. Kim, T-Y. Kim, S. W. Nam, M. Mitoraj, Ł. Piekoś, A. Michalak, S-J. Hwang, S. O. Kang, *J. Am. Chem. Soc.* **2010**, *132*, 9954.
- [24] E. Rangel, E. Sansores, E. Vallejo, A. Hernandez-Hernandez and P. A. Lopez-Pérez, *Phys. Chem. Chem. Phys.* **2016**, *18*, 33158.
- [25] T. Gómez, E. Florez, J. A. Rodriguez, F. Illas, *J. Phys. Chem. C* **2011**, *115*, 11666.
- [26] R. V. Gonçalves, L. L. R. Vono, R. Wojcieszak, C. S. B. Dias, H. Wender, E. Teixeira-Neto, L. M. Rossi, *Appl. Catal. B Environ.* **2017**, *209*, 240.
- [27] T. N. Gieshoff, U. Chakraborty, M. Villa, A. Jacobi von Wangelin, *Angew. Chem.* **2017**, *129*, 1.
- [28] F. R. Lucci, M. T. Darby, M. F. G. Mattera, C. J. Ivimey, A. J. Therrien, A. Michaelides, M. Stamatakis, E. C. H. Sykes, *J. Phys. Chem. Lett.* **2016**, *7*, 480.
- [29] E. Florez, T. Gomez, P. Liu, J. A. Rodriguez, F. Illas, *ChemCatChem* **2010**, *2*, 1219.
- [30] M. Haruta, N. Yamada, T. Kobayashi, S. Lijima, *J. Catal.* **1989**, *115*, 301.
- [31] B. Schaefer, R. Pal, N. S. Khetrpal, M. Amsler, A. Sadeghi, V. Blum, X. C. Zeng, S. Goedecker, L-S. Wang, *ACS Nano* **2014**, *8*, 7413.
- [32] P. Ghosh, M. F. Camellone, S. Fabris, *J. Phys. Chem. Lett.* **2013**, *4*, 2256.
- [33] F. Ferraro, J. F. Pérez-Torres, C. Z. Hadad, *J. Phys. Chem. C* **2015**, *119*, 7755.
- [34] Y. Pan, Y. Cui, C. Stiehler, N. Nilius, H-J. Freund, *J. Phys. Chem. C* **2013**, *117*, 21879.
- [35] N. Moreno, F. Ferraro, E. Florez, C. Z. Hadad, A. Restrepo, *J. Phys. Chem. A* **2016**, *120*, 1698.
- [36] K. Balasubramanian, P. Y. Feng, M. Z. Liao, *J. Chem. Phys.* **1989**, *91*, 3561.
- [37] L. M. Ghiringhelli, P. Gruene, J. T. Lyon, D. M. Rayner, G. Meijer, A. Fielicke, M. Scheffler, *New J. Phys.* **2013**, *15*, 083003.
- [38] P. Gruene, B. Butschke, J. T. Lyon, D. M. Rayner, A. Fielicke, *Z. Phys. Chem.* **2014**, *228*, 337.
- [39] F. Pérez, C. Z. Hadad, A. Restrepo, *Int. J. Quantum Chem.* **2008**, *108*, 1653.
- [40] F. Perez, E. Florez, C. Z. Hadad, P. Fuentealba, A. Restrepo, *J. Phys. Chem. A* **2008**, *112*, 5749.
- [41] C. Ibarguen, M. Manrique-Moreno, C. Z. Hadad, J. David, A. Restrepo, *Phys. Chem. Chem. Phys.* **2013**, *15*, 3203.
- [42] A. Zapata-Escobar, M. Manrique-Moreno, D. Guerra, C. Z. Hadad, A. Restrepo, *J. Chem. Phys.* **2014**, *140*, 184312.
- [43] S. Gómez, A. Restrepo, C. Z. Hadad, *Phys. Chem. Chem. Phys.* **2015**, *17*, 31917.
- [44] E. Flórez, G. Merino, J. L. Cabellos, F. Ferraro, A. Restrepo, C. Z. Hadad, *Theor. Chem. Acc.* **2016**, *135*, 216.

- [45] M. J. Frisch, G. W. Trucks, H. B. Schlegel, G. E. Scuseria, M. A. Robb, J. R. Cheeseman, G. Scalmani, V. Barone, G. A. Petersson, H. Nakatsuji, X. Li, M. Caricato, A. Marenich, J. Bloino, B. G. Janesko, R. Gomperts, B. Mennucci, H. P. Hratchian, J. V. Ortiz, A. F. Izmaylov, J. L. Sonnenberg, D. Williams-Young, F. Ding, F. Lipparini, F. Egidi, J. Goings, B. Peng, A. Petrone, T. Henderson, D. Ranasinghe, V. G. Zakrzewski, J. Gao, N. Rega, G. Zheng, W. Liang, M. Hada, M. Ehara, K. Toyota, R. Fukuda, J. Hasegawa, M. Ishida, T. Nakajima, Y. Honda, O. Kitao, H. Nakai, T. Vreven, K. Throssell, J. A. Montgomery, Jr, J. E. Peralta, F. Ogliaro, M. Bearpark, J. J. Heyd, E. Brothers, K. N. Kudin, V. N. Staroverov, T. Keith, R. Kobayashi, J. Normand, K. Raghavachari, A. Rendell, J. C. Burant, S. S. Iyengar, J. Tomasi, M. Cossi, J. M. Millam, M. Klene, C. Adamo, R. Cammi, J. W. Ochterski, R. L. Martin, K. Morokuma, O. Farkas, J. B. Foresman, D. J. Fox, *Gaussian 09, Revision C.01*, Gaussian Inc, Wallingford, Connecticut **2010**.
- [46] ADF2012, *Theoretical Chemistry*, Vrije Universiteit, Amsterdam **2012**.
- [47] E. van Lenthe, E. J. Baerends, J. G. Snijders, *J. Chem. Phys.* **1994**, *101*, 9783.
- [48] J. P. Perdew, Y. Wang, *Phys. Rev. B* **1992**, *45*, 13244.
- [49] J. P. Perdew, J. A. Chevary, S. H. Vosko, K. A. Jackson, M. R. Pederson, D. J. Sing, C. Fiolhais, *Phys. Rev. B* **1992**, *46*, 6671.
- [50] F. Weigend, R. Ahlrichs, *Phys. Chem. Chem. Phys.* **2005**, *7*, 3297.
- [51] F. Weigend, *Phys. Chem. Chem. Phys.* **2006**, *8*, 1057.
- [52] X. Li, M. J. Frisch, *J. Chem. Theory Comput.* **2006**, *2*, 835.
- [53] H. P. Hratchian, H. B. Schlegel, *J. Chem. Phys.* **2004**, *120*, 9918.
- [54] C. Peng, H. B. Schlegel, *Israel J. Chem.* **1993**, *33*, 449.
- [55] F. Weinhold, C. R. Landis, *Discovering Chemistry with Natural Bond Orbitals*, Wiley-VCH, Hoboken, NJ **2012**.
- [56] E. D. Glendening, J. K. Badenhop, A. E. Reed, J. E. Carpenter, J. A. Bohman, C. M. Morales, C. R. Landis, F. Weinhold, *NBO 6.0.*, Theoretical Chemistry Institute, University of Wisconsin, Madison **2013**.
- [57] R. Bader, *Atoms in Molecules: A Quantum Theory*, Oxford University Press, USA **1994**.
- [58] D. Y. Zubarev, A. I. Boldyrev, *Phys. Chem. Chem. Phys.* **2008**, *10*, 5207.
- [59] K. B. Wiberg, *Tetrahedron* **1968**, *24*, 1083.
- [60] A. Todd, T. K. Keith, *AIMAll Version 13.05.06*, Gristmill Software, Overland Park, Kansas **2013**.
- [61] T. Lu, F. Chen, *J. Comput. Chem.* **2012**, *33*, 580.
- [62] E. Clementi, D. L. Raimond, W. P. Reinhardt, *J. Chem. Phys.* **1967**, *47*, 1300.
- [63] P. Pyykkö, M. Atsumi, *Chemistry* **2009**, *15*, 186.
- [64] E. Osorio, F. Ferraro, C. Z. Hadad, W. A. Rabanal-Leon, W. Tiznado, *Theor. Chem. Acc.* **2016**, *135*, 212.
- [65] E. D. Glendening, C. R. Landis, F. Weinhold, *Wiley Interdiscip. Rev. Comput. Mol. Sci.* **2012**, *2*, 1.

SUPPORTING INFORMATION

Additional Supporting Information may be found online in the supporting information tab for this article.

How to cite this article: Mejía L, Ferraro F, Osorio E, Hadad CZ. Activation and diffusion of ammonia borane hydrogen on gold tetramers. *Int J Quantum Chem.* 2017;e25567. <https://doi.org/10.1002/qua.25567>